ISSN 1007-9327 (print)
ISSN 2219-2840 (online)

# World Journal of *Gastroenterology*

*World J Gastroenterol* 2018 May 14; 24(18): 1925-2046

Published by Baishideng Publishing Group Inc

World Journal of Gastroenterology

Contents

Weekly Volume 24 Number 18 May 14, 2018

**Contents**

*World Journal of Gastroenterology*
**Volume 24 Number 18 May 14, 2018**

## ABOUT COVER

Editorial board member of *World Journal of Gastroenterology*, Andrew Stewart Day, MD, Professor, Paediatrics Department, University of Otago, Christchurch 8041, New Zealand

## AIMS AND SCOPE

*World Journal of Gastroenterology* (*World J Gastroenterol*, *WJG*, print ISSN 1007-9327, online ISSN 2219-2840, DOI: 10.3748) is a peer-reviewed open access journal. *WJG* was established on October 1, 1995. It is published weekly on the 7th, 14th, 21st, and 28th each month. The *WJG* Editorial Board consists of 642 experts in gastroenterology and hepatology from 59 countries.

The primary task of *WJG* is to rapidly publish high-quality original articles, reviews, and commentaries in the fields of gastroenterology, hepatology, gastrointestinal endoscopy, gastrointestinal surgery, hepatobiliary surgery, gastrointestinal oncology, gastrointestinal radiation oncology, gastrointestinal imaging, gastrointestinal interventional therapy, gastrointestinal infectious diseases, gastrointestinal pharmacology, gastrointestinal pathophysiology, gastrointestinal pathology, evidence-based medicine in gastroenterology, pancreatology, gastrointestinal laboratory medicine, gastrointestinal molecular biology, gastrointestinal immunology, gastrointestinal microbiology, gastrointestinal genetics, gastrointestinal translational medicine, gastrointestinal diagnostics, and gastrointestinal therapeutics. *WJG* is dedicated to become an influential and prestigious journal in gastroenterology and hepatology, to promote the development of above disciplines, and to improve the diagnostic and therapeutic skill and expertise of clinicians.

## INDEXING/ABSTRACTING

*World Journal of Gastroenterology* (*WJG*) is now indexed in Current Contents®/Clinical Medicine, Science Citation Index Expanded (also known as SciSearch®), Journal Citation Reports®, Index Medicus, MEDLINE, PubMed, PubMed Central and Directory of Open Access Journals. The 2017 edition of Journal Citation Reports® cites the 2016 impact factor for *WJG* as 3.365 (5-year impact factor: 3.176), ranking *WJG* as 29th among 79 journals in gastroenterology and hepatology (quartile in category Q2).



NAME OF JOURNAL
*World Journal of Gastroenterology*

ISSN
ISSN 1007-9327 (print)
ISSN 2219-2840 (online)

LAUNCH DATE
October 1, 1995

FREQUENCY
Weekly



EDITORIAL OFFICE
Ze-Mao Gong, Director
*World Journal of Gastroenterology*
Baishideng Publishing Group Inc
7901 Stoneridge Drive, Suite 501,
Pleasanton, CA 94588, USA
Telephone: +1-925-2238242
Fax: +1-925-2238243
E-mail: editorialoffice@wjgnet.com
Help Desk: http://www.f6publishing.com/helpdesk
http://www.wjgnet.com

PUBLISHER
Baishideng Publishing Group Inc
7901 Stoneridge Drive, Suite 501,
Pleasanton, CA 94588, USA
Telephone: +1-925-2238242
Fax: +1-925-2238243
E-mail: bpgoffice@wjgnet.com
Help Desk: http://www.f6publishing.com/helpdesk
http://www.wjgnet.com

PUBLICATION DATE
May 14, 2018



INSTRUCTIONS TO AUTHORS
Full instructions are available online at http://www.wjgnet.com/bpg/gerinfo/204

ONLINE SUBMISSION
http://www.f6publishing.com

World Journal of Gastroenterology

Submit a Manuscript: http://www.f6publishing.com

*World J Gastroenterol* 2018 May 14; 24(18): 2024-2035

DOI: 10.3748/wjg.v24.i18.2024

ISSN 1007-9327 (print) ISSN 2219-2840 (online)

ORIGINAL ARTICLE

Clinical Trials Study

# Quantitative assessment of hepatic fibrosis in chronic hepatitis B and C: T1 mapping on Gd-EOB-DTPA-enhanced liver magnetic resonance imaging

Shen Pan, Xiao-Qi Wang, Qi-Yong Guo

Shen Pan, Qi-Yong Guo, Department of Radiology, Shengjing Hospital of China Medical University, Shenyang 110004, Liaoning Province, China

Xiao-Qi Wang, Department of Clinical Science, Philips Healthcare, Beijing 100600, China

ORCID number: Shen Pan (0000-0002-6267-1964); Xiao-Qi Wang (0000-0001-6357-0420); Qi-Yong Guo (0000-0003-0046-0712).

Author contributions: Pan S and Wang XQ contributed to this work; Pan S and Guo QY designed research; and Pan S wrote the paper.

Supported by National Natural Science Foundation of China, No. 81771893, No. 81771802, No. 81471718 and No. 81401376; and Outstanding Youth Foundation of China Medical University, No. YQ20160005.

Institutional review board statement: This study was reviewed and approved by the Shengjing Hospital of China Medical University Institution Review Board, ID# 2014PS103K.

Informed consent statement: The authors of this paper guarantee that all study participants or their legal guardian(s) provided informed written consent about personal and medical data collection prior to study enrolment.

Conflict-of-interest statement: There are no conflict of interests in relation to this manuscript.

Data sharing statement: There are no additional data available in relation to this manuscript.



Manuscript source: Unsolicited manuscript

Correspondence to: Qi-Yong Guo, MD, Professor, Department of Radiology, Shengjing Hospital of China Medical University, No. 36 Sanhao Street, Heping District, Shenyang 110004, Liaoning Province, China. guoqysj@126.com
Telephone: +86-13840231345
Fax: +86-96615-73219

Received: March 9, 2018
Peer-review started: March 9, 2018
First decision: March 29, 2018
Revised: April 6, 2018
Accepted: April 15, 2018
Article in press: April 15, 2018
Published online: May 14, 2018

## Abstract

***AIM***

To assess the accuracy of Look-Locker on gadolinium ethoxybenzyl diethylenetriamine pentaacetic acid (Gd-EOB-DTPA)-enhanced magnetic resonance imaging (MRI) for staging liver fibrosis in chronic hepatitis B/C (CHB/C).

***METHODS***

We prospectively included 109 patients with CHB or CHC who underwent a 3.0-Tesla MRI examination, including T1-weighted and Look-Locker sequences for T1 mapping. Hepatocyte fractions (HeF) and relaxation time reduction rate (RE) were measured for staging liver fibrosis. A receiver operating characteristic analysis using the area under the receiver operating characteristic curve (AUC) was used to compare the

diagnostic performance in predicting liver fibrosis between HeF and RE.

***RESULTS***

A total of 73 patients had both pathological results and MRI information. The number of patients in each fibrosis stage was evaluated semiquantitatively according to the METAVIR scoring system: F0, *n* = 23 (31.5%); F1, *n* = 19 (26.0%); F2, *n* = 13 (17.8%); F3, *n* = 6 (8.2%), and F4, *n* = 12 (16.4%). HeF by EOB enhancement imaging was significantly correlated with fibrosis stage ($r$ = -0.808, $P$ < 0.05). AUC values for diagnosis of any (≥ F1), significant (≥ F2) or advanced (≥ F3) fibrosis, and cirrhosis (F4) using HeF were 0.837 (0.733-0.913), 0.890 (0.795-0.951), 0.957 (0.881-0.990), and 0.957 (0.882-0.991), respectively. HeF measurement was more accurate than use of RE in establishing liver fibrosis staging, suggesting that calculation of HeF is a superior noninvasive liver fibrosis staging method.

***CONCLUSION***

A T1 mapping-based HeF method is an efficient diagnostic tool for the staging of liver fibrosis.

**Key words:** Liver fibrosis; Gd-EOB-DTPA; Look-Locker; Hepatocyte fraction; Liver function; Magnetic resonance imaging relative enhancement



**Core tip:** T1 mapping using the Look-Locker method with gadolinium ethoxybenzyl diethylenetriamine pentaacetic acid-enhanced magnetic resonance imaging at 3-Tesla by calculating the hepatocyte fraction is an efficient method for the assessment of liver fibrosis in patients with chronic hepatitis B and C, and this method is superior to using reduction rate.

Pan S, Wang XQ, Guo QY. Quantitative assessment of hepatic fibrosis in chronic hepatitis B and C: T1 mapping on Gd-EOB-DTPA-enhanced liver magnetic resonance imaging. *World J Gastroenterol* 2018; 24(18): 2024-2035 Available from: URL: http://www.wjgnet.com/1007-9327/full/v24/i18/2024.htm DOI: http://dx.doi.org/10.3748/wjg.v24.i18.2024

## INTRODUCTION

Chronic hepatitis B (CHB) and chronic hepatitis C (CHC) are major health problems[1,2] and important factors globally in the development of hepatic fibrosis and even cirrhosis[3,4]. Liver fibrosis is a diffuse pathological change caused by chronic liver disease. As fibrosis progresses, it leads to cirrhosis and even cancer[5]. Early diagnosis and monitoring of liver fibrosis, and intervention with timely and effective treatments, are critical for patients with liver disease.

At present, liver biopsy is the gold standard for diagnosis of liver fibrosis. Tissue acquisition from a liver can be performed by endoscopic ultrasound-guided fine-needle aspiration[6-8], particularly for the left lobe[9,10]. This method is invasive, with a risk of bleeding and increased tissue injury, and repeatability of the examination is poor[11,12]. Therefore, noninvasive, comprehensive and accurate methods of diagnosing liver fibrosis are required. In recent years, noninvasive methods have been increasingly used, such as serological examination[13], ultrasound-based elastography[14], diffusion-weighted imaging (DWI)[15], magnetic resonance enterography (MRE)[16], T1 rho[17] and texture analysis[18].

Gadolinium ethoxybenzyl diethylenetriamine pentaacetic acid (Gd-EOB-DTPA) is a liver-specific contrast agent that has a higher hepatocellular uptake rate than the traditionally used gadobenate dimeglumine (Gd-BOPTA)[19]. In previous studies, Gd-EOB-DTPA-enhanced magnetic resonance imaging (MRI) was mainly used to diagnose focal liver lesions, especially hepatocellular carcinomas, and even on functional MR cholangiography[20-22]. It has been shown that the intracellular transport mechanisms of Gd-EOB-DTPA are mediated by organic anion-transporting polypeptides (OATPs)[23]. Liver fibrosis obstructs the delivery of Gd-EOB-DTPA to hepatic cell surface transporters[24], contributing to a decline in OATP expression in the diseased liver[25], and consequently causing a decline in the T1-shortening effect of gadoxetic acid[26].

Recording liver parenchymal T1 values before and after drug administration allows the T1 relaxation time reduction rate (RE) to be calculated, reflecting the functional hepatocyte-specific uptake of gadoxetic acid and, thus, the state of the liver[27]. This method has been shown to have accurate diagnostic value in the assessment of liver fibrosis and is based on the traditional diagnostic method of Gd-EOB-DTPA-enhanced MR.

Use of T1 mapping technology is a noninvasive, quantitative method for determining tissue T1 relaxation time. After liver fibrosis, excessive accumulation of extracellular matrix proteins occur, leading to T1 relaxation time changes in fibrotic tissues. Therefore, T1 mapping is theoretically applicable to studies of liver fibrosis, such as the variable flip angle T1 mapping technique[28], which has been shown to be effective in diagnosing liver fibrosis.

T1 mapping using the Look-Locker method is one of the fastest, most efficient and reliable approaches to T1 quantification[29]. We proposed a method based on a simple pharmacokinetic model and ΔR1 values to calculate a hepatocyte fraction (HeF). In this method, changes to R1 in liver and spleen after EOB administration are calculated to obtain the HeF. In previous studies, the Look-Locker technique has mostly been used in the assessment of myocardial fibrosis and liver function[30]. However, its application in the clinical diagnosis of liver fibrosis has not yet been reported.

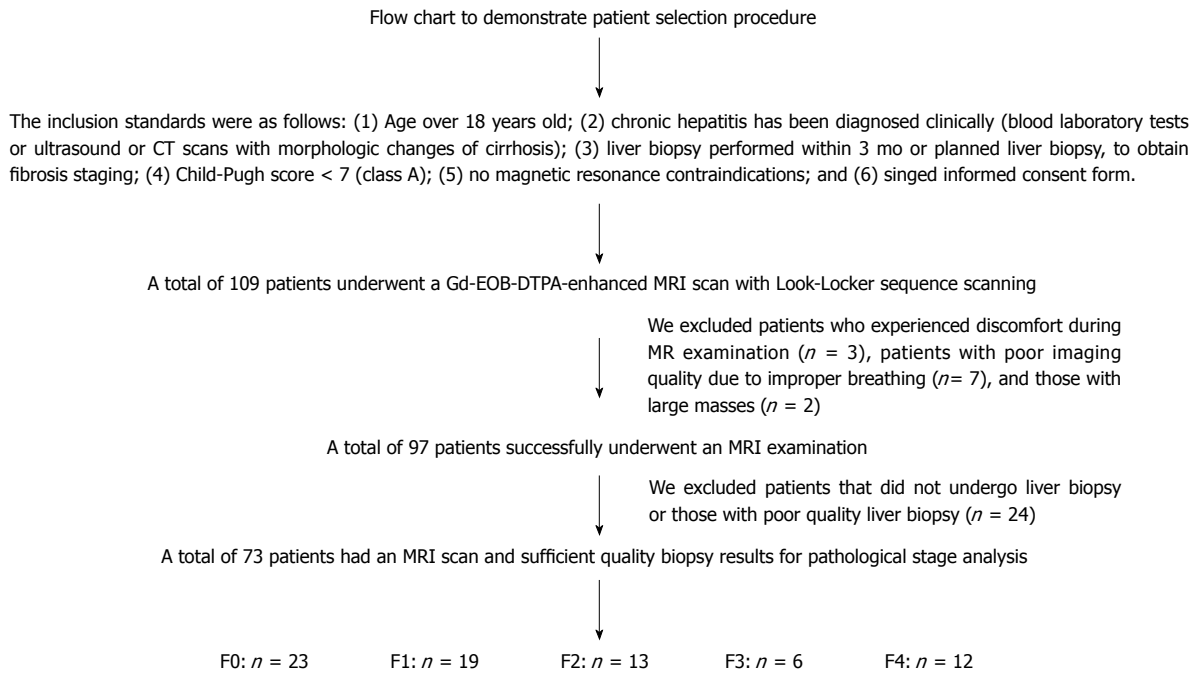


**Figure 1 Flow chart to demonstrate the patient selection procedure.**

Therefore, we proposed a working hypothesis that it was possible to diagnose liver fibrosis by calculating the HeF in the Look-Locker sequence by measuring Gd-EOB-DTPA-enhanced T1 signal intensity, and that this method would be superior to using RE. The purpose of this study, based on pathologic gold standards, was to quantitatively assess the level of hepatic fibrosis in hepatitis B and C patients by calculating the HeF and to compare the results with traditional T1-enhanced test parameters with the aim of establishing a novel noninvasive diagnosis method for liver fibrosis.

## MATERIALS AND METHODS

This cross-sectional, prospective study was performed between August 2016 and June 2017. The study was approved by our institutional review board, and written informed consent was obtained from the participants prior to the study.

### *Patient population*

The subjects of the study were patients with suspected or known chronic liver disease attending our hospital's infectious disease department. The inclusion criteria were as follows: (1) > 18-years-old; (2) chronic hepatitis diagnosed clinically (blood laboratory tests, ultrasound, or computed tomography scans showing morphological cirrhotic changes); (3) liver biopsy performed within 3 mo prior to the study or liver biopsy planned to obtain fibrosis staging; (4) Child-Pugh score < 7 (class A); (5) no MR contraindications; and (6) signed informed consent.

A total of 109 patients met the inclusion criteria, with 84 having CHB and 25 having CHC. We excluded 3 patients due to discomfort during the MR examination, 7 patients due to poor imaging quality from improper breathing, and 2 with a mass that was too large. The remaining patients ($n$ = 97) were scheduled for a liver biopsy within 1 wk of the MRI. Of these 97, 20 did not undergo liver biopsy, and 4 were excluded due to poor liver biopsy quality. The standards for patient inclusion and exclusion are shown in Figure 1.

### *MRI acquisition*

MR images were obtained with a 3-Tesla MRI system (Ingenia; Phillips Healthcare, Best, Netherlands) using a 32-channel torso phased-array coil. Patients were instructed to fast without water intake for 4-6 h before MR scanning. Before the examination, patients were trained to reduce breathing frequency or an abdominal binder was used to limit breathing frequency, to reduce interference during image acquisition.

A volume of 0.025 mmol/kg Gd-EOB-DTPA (Bayer Healthcare, Berlin, Germany) was administered at a rate of 1-2 mL/s. Following this, 30 mL saline was administered to flush the residual contrast reagent from the injection tube. T1WI and Look-Locker sequences were obtained twice (before and after the Gd-EOB-DTPA administration). To obtain T1 relaxation time, enhanced images were recorded 18 min after the Gd-EOB-DTPA injection.

The T1WI sequence was obtained using the scan parameters of FOV = 356 mm × 262 mm; slice thickness = 7 mm, 24 slices, in-plane resolution = 1.6 mm × 1.96 mm, matrix = 220 × 133, TR/TE = 12/2.3 ms, and band width = 361.9 kHz. Two-dimensional (2D) T1 maps were obtained using Look-Locker sequencing before and 20 min after the Gd-EOB-DTPA administration[31]. A three-

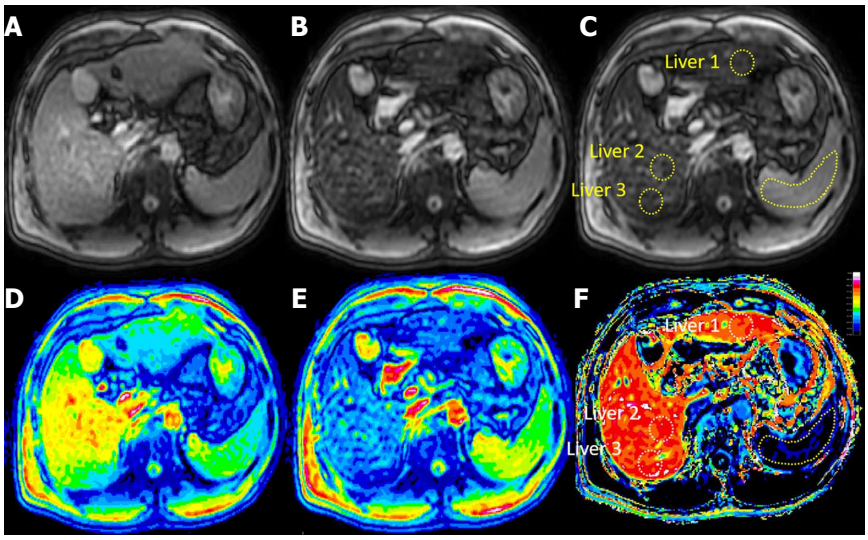


**Figure 2 Precontrast (A, D) and postcontrast (B, E) T1 maps in a 72-year-old male with a METAVIR score of F4.** The hand-drawn regions of interest of the liver and spleen are shown (C; dotted closed curves). HeF image (F) is shown, and HeF liver 1, HeF liver 2 and HeF liver 3 values were 68.13%, 72.46% and 70.45%, respectively, resulting in a HeF liver average of 70.34%. HeF: Hepatocyte fraction.

lead vector cardiogram was used for electrocardiogram gating. The T1 map was calculated from the Look-Locker sequence using the scan parameters of 2D image with single slice, TE/TR = 1/6 ms, 3.5 mm × 3.5 mm × 8 mm acquisition resolution, and 1.37 mm × 1.37 mm × 8 mm for recon, FA = 7°, two shots TFE with TFE factor 16, shot interval = 5 s for full T1 relaxation, SENSE factor = 2, and scan time = 15 s, with breath holding.

T1 maps were then automatically calculated using HepFract work-in-progress software (Phillips Healthcare).

### *Assessment of pathological specimens*

Liver biopsy was performed under ultrasound guidance using an intercostal approach with a 14G disposable needle (MN1420; Bard Biopsy Systems, Tempe, AZ, United States) under local anesthesia. Liver specimens < 15 mm or containing < 11 portal tracts were excluded. Pathological sections of the biopsies were stained using the Masson method. Each pathologic section was read by two doctors with more than 10 years of pathologic diagnostic experience and who were unaware of the patient serological or imaging diagnosis. If the opinion of the two pathologists differed, a final diagnosis was reached by, or after, discussion with a more senior pathologist.

Fibrosis stage was evaluated semiquantitatively according to the METAVIR scoring system[32], with grading on a 5-point scale as follows: F0, no fibrosis; F1, fibrous portal expansion but without septa formation; F2, few bridges or septa; F3, numerous septa formation without cirrhosis; and F4, cirrhosis[33].

### *MRI analysis*

As mentioned above, two doctors with more than 10 years of experience in the diagnosis of abdominal imaging - both of whom were unaware of the patient's laboratory results, pathologic grade or clinical diagnosis prior to measurement - assessed the MR images, with any inconsistency finalized by a senior clinician.

The scanned pre- and post Look-Locker images were saved in PAR-REC format, with the files imported into the HepFract processing software (Philips Scientific Software). Regions of interest (ROIs) were defined manually. A spleen ROI of about 4-5 $cm^2$ was drawn first, and three ROI of approximately 2-3 $cm^2$ were selected and marked in the liver parenchyma, two in the right lobe and three in the left (Figure 2), avoiding visible macroscopic vascular areas, the bile duct and the liver edge. No selection was made if the left lobe was too small or the image quality was insufficient. The HeF was calculated using the following formulas:

R1 change after EOB in both liver and spleen:

$$\Delta R1_{Liver} = 1 - \varphi_{Liver} \times \Delta R1_{Hepatobiliary} + \varphi_{Liver} \times \Delta R1_{BloodEES}$$

and

$$\Delta R1_{Spleen} = \varphi_{Spleen} \times \Delta R1_{BloodEES}$$

Where $\varphi$ = total tissue water content [blood and extracellular space (EES)], $\varphi_{Liver}$ = 0.23, and $\varphi_{Spleen}$ = 0.3).

HeF:

$$(\Delta R1_{Hepatobiliary})/(\Delta R1_{Hepatobiliary} + \Delta R1_{BloodEES}) \times 100\ (\%),$$

Where $\Delta R1_{Hepatobiliary}$ = the T1 relaxation rate change of the liver parenchyma ROI before and after contrast reagent administration and $\Delta R1_{BloodEES}$ = the T1 relaxation rate change of blood, which was estimated based on the comparison of T1 relaxation rate of spleen parenchyma and liver parenchyma ROIs.

RE image processing was performed using DICOM Viewer R3.0 SP3 software (Philips). Images at the same Look-Locker level were preferred. Three ROIs were selected from the T1 liver images before and after Gd-EOB-DTPA administration. The ROIs were selected according to anatomical signs and the ROI positions of the Look-Locker images as far as possible. Figure 3 shows

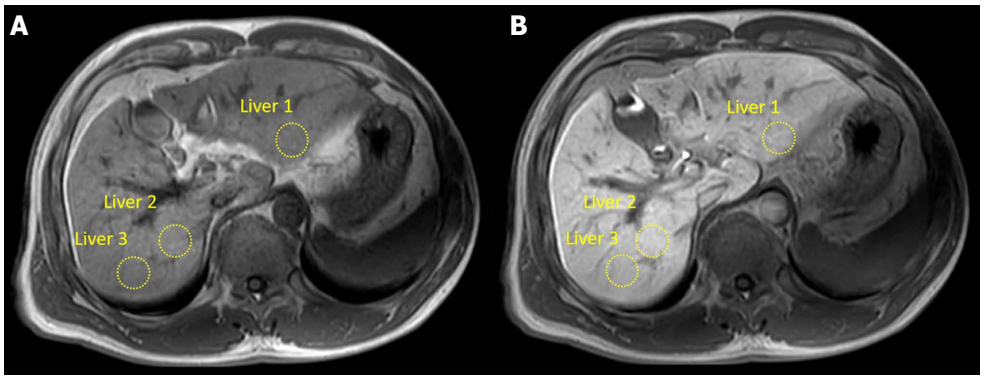


**Figure 3 Precontrast (A) and postcontrast (B) T1-weighted images in a 72-year-old male with a METAVIR score of F4.** The hand-drawn regions of interest of the liver are shown (dotted closed curves). RE was 0.45. RE: Reduction rate of T1 relaxation time.

**Table 1 Patients' characteristics *n* %**

| Characteristic | No fibrosis, *n* = 23 | Liver fibrosis, *n* = 50 | All, *n* = 73 |
|---|---|---|---|
| Age in yr | 39.5 ± 11.1 | 41.3 ± 12.5 | 40.8 ± 12.1 |
| Sex | | | |
| Male | 17 (74) | 30 (60) | 47 (64) |
| Female | 6 (26) | 20 (40) | 26 (36) |
| Height in m | 1.72 ± 0.09 | 1.70 ± 1.21 | 1.71 ± 1.15 |
| Weight in kg | 77.21 ± 17.32 | 78.23 ± 16.12 | 78.10 ± 16.64 |
| BMI in kg/m$^2$ | 24.09 ± 4.91 | 22.06 ± 4.57 | 23.73 ± 4.65 |
| CHB | 21 (34) | 41 (66) | 62 (85) |
| CHC | 2 (18) | 9 (82) | 11 (15) |

Data are presented as *n* (%) or mean ± SD. BMI: Body mass index; CHB: Chronic hepatitis B; CHC: Chronic hepatitis C.

ROI selection for the RE method. The RE was calculated according to the formula:

RE = [(Post-Pre)/Pre] × 100 (%),

Where Pre and Post were the average signal intensity of liver parenchyma ROIs before and after Gd-EOB-DTPA administration.

Finally, the averages of the HeF, RE, Post, and Pre calculations for the three ROIs were calculated.

### *Statistical analysis*

After testing for normality with the Shapiro-Wilk test, HeF, RE, Post, and Pre were expressed as the mean ± standard deviation. One-way analysis of variance followed by Bonferroni's/Tamhane's T2 post-hoc comparison were performed to compare the means. Spearman's rank correlation coefficient (*r*) was used to show the correlation between HeF, RE, Post, Pre, and histological scores.

We performed receiver operating characteristic (ROC) analysis of the different stages of fibrosis and area under the ROC curve (AUC) analysis was used to evaluate the following classifications: F0 *vs* F1-F4 (≥ F1); F0-F1 *vs* F2-F4 (≥ F2); F0-F2 *vs* F3-F4 (≥ F3); and F0-F3 *vs* F4, using Pre, Post, the RE of the hepatobiliary phase and the HeF, based on Look-Locker. The optimal discrimination thresholds for RE and HeF were determined by maximizing the sums of sensitivity and specificity. The cut-off values, sensitivity, specificity, negative predictive value, positive predictive value, positive likelihood ratio and negative likelihood ratio were calculated. Comparisons of AUCs were carried out using the method proposed by DeLong *et al*[34].

Data analysis was performed with SPSS software, version 17.0 (SPSS, Chicago, IL, United States) and MedCalc version 7.4.2.0 (MedCalc Software, Mariakerke, Belgium) statistical software. A $P$ value < 0.05 was considered significant.

## RESULTS

### *Patient characteristics*

The epidemiological characteristics of the enrolled patients, based on the presence or absence of fibrosis, are summarized in Table 1. We included a total of 73 patients [47 (64%) male and 26 (36%) female] who were eligible for inclusion on histopathological findings. Of these, 62 (85%) were infected with CHB and 11 (15%) were infected with CHC. Patient age ranged from 19-67 years (40.8 ± 12.1 years). Among them, there were 23 patients (31.5%) without fibrosis and 50 patients (68.5%) with fibrosis. Mean body mass index was 23.73 ± 4.65 kg/m$^2$ for the overall sample, and 15 of the 73 patients (21%) were overweight/obese (> 25 kg/m$^2$), 9 with CHB and 6 with CHC.

### *Differences in MRI at different levels of fibrosis*

The average Post, RE and HeF (%) in patients without fibrosis was 356 ± 44, 0.94 ± 0.18 and 88.77 ± 5.10, respectively, which were significantly lower than in patients with fibrosis (Post: 331 ± 45; RE: 0.79 ± 0.23; HeF (%): 76.31 ± 11.23), and these values were significantly different between fibrotic and non-fibrotic patients ($P$ = 0.037, 0.009 and < 0.001, respectively). Pre was not significantly different between patients with or without fibrosis ($P$ = 0.235). The Pre, Post, RE and HeF (%) (mean ± SD) in patients with different grades of fibrosis are summarized in Table 2.

Post, RE and HeF were significantly different among

**Table 2 Pre, Post, reduction rate of T1 relaxation time, and hepatocyte fraction (%) of patients at different METAVIR fibrosis stages**

| Fibrosis stage, (METAVIR) | F0, *n* = 23 | F1, *n* = 19 | F2, *n* = 13 | F3, *n* = 6 | F4, *n* = 12 | Total, *n* = 73 |
|---|---|---|---|---|---|---|
| Mean pre-T1 liver | 180 ± 28 | 188 ± 19 | 174 ± 17 | 192 ± 22 | 200 ± 24 | 186 ± 24 |
| Mean post-T1 liver | 356 ± 44 | 355 ± 38 | 316 ± 34 | 336 ± 43 | 305 ± 50 | 338 ± 46 |
| RE | 0.94 ± 0.18 | 0.89 ± 0.20 | 0.94 ± 0.16 | 0.71 ± 0.17 | 0.52 ± 0.15 | 0.84 ± 0.23 |
| HeF (%) | 88.77 ± 5.10 | 84.23 ± 6.99 | 79.71 ± 8.09 | 70.90 ± 7.27 | 62.80 ± 7.01 | 80.24 ± 11.30 |

Data are presented as mean ± SD. HeF: Hepatocyte fraction; RE: Reduction rate of T1 relaxation time.

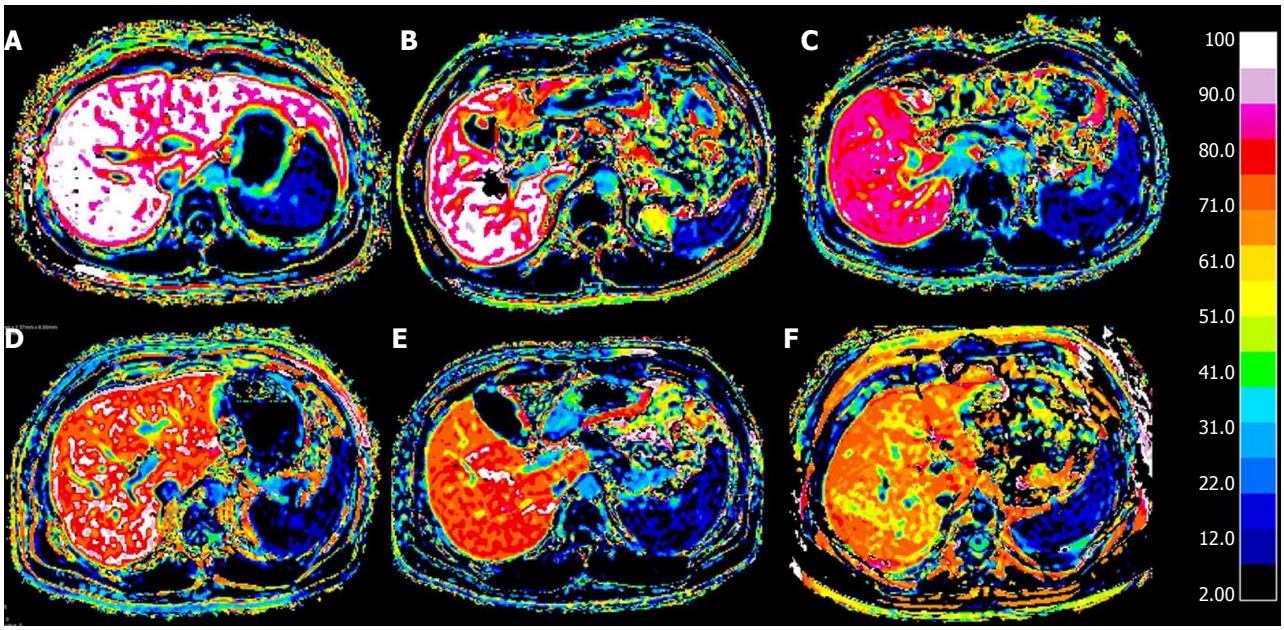


**Figure 4 Representative images from patients with liver fibrosis at F0-F4 METAVIR stages.** A: F0, HeF = 97.16%; B: F1, HeF = 89.21%; C: F2, HeF = 79.92%; D: F2, HeF = 72.94%; E: F3, HeF= 69.17%; F: F4, HeF = 62.43%. HeF: Hepatocyte fraction.

different grades of liver fibrosis (all $P < 0.05$). In the comparison of HeF in different groups of patients with different levels of fibrosis, each pair comparison was significantly different ($P < 0.001$), except for F1 and F2 (F1 *vs* F2 = 84.23 ± 6.99 *vs* 79.71 ± 8.09, $P = 0.065$). RE was not significantly different between the comparison groups F0 *vs* F1, F0 *vs* F2, and F1 *vs* F2 ($P = 0.365$, 0.490, and 0.912, respectively), but was significantly different between other comparison groups ($P < 0.05$). Post was statistically significantly different between patients with liver cirrhosis (F4) and patients without liver fibrosis (F0) (F4 *vs* F0 = 356 ± 44 *vs* 305 ± 50, $P < 0.001$), and was not significantly different between any other comparison groups ($P > 0.05$). Pre was not significantly different among different levels of liver fibrosis ($P > 0.05$). Figure 4 shows the HeF images in different stages of liver fibrosis.

### Correlation analysis

RE and HeF were not correlated with body mass index or age (Spearman's correlation test, $r = 0.034$ and 0.247, $P = 0.847$ and 0.071, respectively), and did not differ between males and females (RE: 0.81 ± 0.27 *vs* 0.83 ± 0.16; HeF (%): 84.29 ± 8.17 *vs* 86.29 ± 6.10; both $P > 0.05$ for the independent samples *t*-test).

HeF and RE showed a strong correlation with fibrosis stage (RE: $r = -0.773$ (-0.852 to 0.661); HeF: $r = 0.808$ (-0.875 to 0.709); both $P < 0.001$). Post was moderately associated with grade of liver fibrosis [$r = -0.525$ (-0.674 to 0.336), $P < 0.001$]. Pre was not related to fibrosis grade [$r = 0.188$ (-0.045 to 0.4003), $P = 0.112$]. Correlation between Pre, Post, RE and HeF (%) with fibrosis ratings is summarized in Table 3 and Figure 5. RE was moderately correlated to HeF [$r = 0.539$ (0.353–0.684), $P < 0.001$].

### ROC analysis

The AUC values, optimal cut-off values and the respective diagnostic performances for liver fibrosis measured by RE and HeF are summarized in Table 4 and Figure 6. The AUC values for HeF and RE were significantly higher than those for Pre and Post for detection of all fibrosis stages ($P < 0.05$). In the AUC comparison of HeF and RE, HeF had slightly higher AUCs than RE for discriminating ⩾ F1 (HeF *vs* RE = 0.837 *vs* 0.678, $P = 0.028$), ⩾ F2 (HeF *vs* RE = 0.890 *vs* 0.723, $P = 0.008$). HeF and RE for ⩾ F3 and F4 stage AUC showed no significant difference (HeF *vs* RE= 0.957 *vs* 0.921, $P = 0.418$; HeF *vs* RE = 0.957 *vs* 0.962,

**Table 3 Correlation of reduction rate of T1 relaxation time, hepatocyte fraction, and METAVIR fibrosis stages**

| | Pre | Post | RE | HeF |
|---|---|---|---|---|
| *r* (95%CI) | 0.188 (-0.045 to 0.4003) | -0.525 (-0.674 to 0.336) | -0.773 (-0.852 to 0.661) | -0.808 (-0.875 to 0.709) |
| *P* value | 0.112 | 0.001 | < 0.001 | < 0.001 |

HeF: Hepatocyte fraction; RE: Reduction rate of T1 relaxation time.

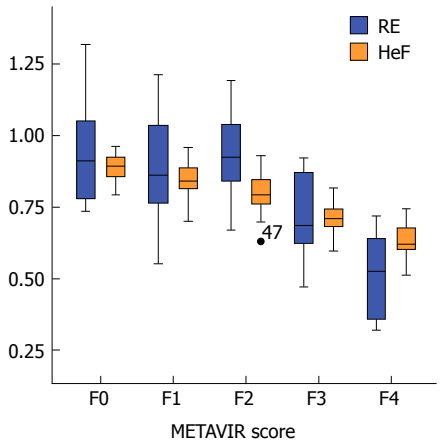


**Figure 5 Box-and-whisker plots of T1 values.** RE and HeF are shown for each METAVIR stage in relation to CHB and CHC. T1 values are reported on the Y-axis, and METAVIR stage of fibrosis is reported on the X-axis. CHB: Chronic hepatitis B; CHC: Chronic hepatitis C; HeF: Hepatocyte fraction; RE: Reduction rate of T1 relaxation time.

respectively).

## DISCUSSION

The results of our study indicated that T1 parameters from pre- or post-contrast T1 maps (HeF) and RE had good diagnostic value in the assessment of CHB, CHC and liver fibrosis. HeF and RE both had good diagnostic performance in advanced liver fibrosis and cirrhosis (⩾ F3 and F4) (AUC > 0.9). In diagnosis at ⩾ F1 and ⩾ F2 stages, HeF was better than RE.

Previous studies have used RE[35], liver-to-spleen ratio[36], contrast enhancement index[37] or dynamic measurements[38] based on Gd-EOB-DTPA-enhanced MRI to quantify parenchymal enhancement. In recent years, T1 mapping technology based on Gd-EOB-DTPA enhancement has been used mainly in the study of liver disease diagnosis. Katsube *et al*[39] first reported that evaluation of hepatic uptake of Gd-EOB-DTPA using T1 mapping of liver parenchyma could help estimate liver function. Kiyohisa *et al*[40] showed similar results in their study, which also demonstrated the diagnostic value of T1 mapping in liver disease.

At present, T1 mapping is used to evaluate the degree of hepatic fibrosis, but only a few studies have focused on liver fibrosis caused by chronic viral hepatitis (CHB, CHC). Li *et al*[28] found that in $CCl_4$-induced liver fibrosis in New Zealand rabbits, using the T1-mapping technique based on a series of liver acquisition volume acceleration sequences, AUCs in ⩾ F1, ⩾ F2 and ⩾ F3 stages from the ROC analysis were 0.803, 0.712 and 0.696, respectively. However, the study did not include F4 data.

Our HeF results were based on clinical patients, which have better reference values than animal experiments, and results for all the fibrosis stages were obtained. Yang *et al*[41] used 3D gradient-echo imaging on a 1.5-T MRI scanner to study volumetric interpolated breath-hold examination in liver fibrosis after CHB infection. They found that reduction in T1 relaxation time 20 min after gadoxetic acid injection (ΔT1, ΔR1%) compared with before injection and the contrast uptake rate ($K_{Hep}$) decreased significantly as the fibrosis score increased. In that study, ΔR1% had the highest correlation with fibrosis stage ($r$ = -0.626), followed by $K_{Hep}$ ($r$ = -0.527), and ΔT1 ($r$ = 0.513).

The above mentioned studies were based on 1.5-T MR, while our images were acquired using 3.0-T MR with better image quality, assisting in image analysis and processing. Banerjee *et al*[42] explored the relationship between corrected T1 parameter (cT1) and hepatic fibrosis Ishak rank, based on a shortened modified Look-Locker inversion (known as shMOLLI) recovery sequence T1 mapping technique, and found that cT1 was strongly correlated with increased liver fibrosis (cT1 *vs* Ishak [$n$ = 84, $r$ = 0.68], AUC of F ⩾ 1 stage = 0.94). While the AUC values for the most of the fibrosis groups were similar to those of our study, the correlation reported by Banerjee *et al*[42] was stronger than what was observed in this study where the AUC value for F ⩾ 1.

Banerjee's study enrolled a total of 84 patients. While the causes of liver fibrosis in their study were from different types of chronic liver disease, 31 cases were caused by virus[42]. A lack of research into viral hepatitis highlights the importance of studying changes in the degree of liver fibrosis caused by different types of liver disease. Sheng *et al*[43] have compared T1 mapping with RE on Gd-EOB-DTPA-enhanced MRI in the field of liver fibrosis assessment. The result showed that Gd-EOB-DTPA-enhanced T1 mapping might provide a reliable diagnostic tool in staging liver fibrosis, whereas it was research performed on rabbits[43]. As our study applies to human, having clinical significance that is superior to animal studies.

Among the T1 mapping techniques, Look-Locker has several advantages. It is efficient compared with conventional techniques, which have only sample one

**Table 4 Performance of the mean reduction rate of T1 relaxation time and hepatocyte fraction for the prediction of METAVIR fibrosis stages according to cut-off values**

| Parameters | ⩾ F1 | ⩾ F2 | ⩾ F3 | = F4 |
|---|---|---|---|---|
| Cut-off | | | | |
| HeF (%) | 82.93 | 79.24 | 74.37 | 74.37 |
| RE | 0.75 | 0.73 | 0.72 | 0.72 |
| AUC | | | | |
| HeF (%) | 0.837 (0.733-0.913) | 0.890 (0.795-0.951) | 0.957 (0.881-0.990) | 0.957 (0.882-0.991) |
| RE | 0.678 (0.559-0.783) | 0.723 (0.606-0.821) | 0.921 (0.834-0.971) | 0.962 (0.889-0.993) |
| Sensitivity, % | | | | |
| HeF(%) | 72.0 (57.5-83.8) | 77.4 (58.9-90.4) | 94.4 (72.7-99.9) | 100.0 (73.5-100.0) |
| RE | 44.0 (30.0-58.7) | 58.1 (39.1-75.5) | 88.9 (65.3-98.6) | 100.0 (73.5-100.0) |
| Specificity, % | | | | |
| HeF (%) | 82.6 (61.2-95.0) | 92.9 (80.5-98.5) | 92.7 (82.4-98.0) | 85.3 (73.8-93.0) |
| RE | 100.0 (85.2-100.0) | 92.9 (80.5-98.5) | 92.7 (82.4-98.0) | 86.9 (75.8-94.2) |
| PPV, % | | | | |
| HeF (%) | 90.0 (76.3-97.2) | 88.9 (70.8-97.6) | 81.0 (58.1-94.6) | 57.1 (34.0-78.2) |
| RE | 100.0 (84.6-100.0) | 85.7 (63.7-97.0) | 80.0 (56.3-94.3) | 60.0 (36.1-80.9) |
| NPV, % | | | | |
| HeF (%) | 57.6 (39.2-74.5) | 84.8 (71.1-93.7) | 98.1 (89.7-100.0) | 100.0 (93.2-100.0) |
| RE | 45.1 (31.1-59.7) | 75.0 (61.1-86.0) | 96.2 (87.0-99.5) | 100.0 (93.3-100.0) |
| PLR | | | | |
| HeF (%) | 4.14 (1.7-10.3) | 10.84 (3.6-32.8) | 12.99 (5.0-33.6) | 6.78 (3.7-12.4) |
| RE | _ | 8.13 (2.6-25.2) | 12.22 (4.7-31.8) | 7.62 (4.0-14.5) |
| NLR | | | | |
| HeF (%) | 0.34 (0.2-0.5) | 0.24 (0.1-0.5) | 0.060 (0.009-0.4) | _ |
| RE | 0.56 (0.4-0.7) | 0.45 (0.3-0.7) | 0.12 (0.03-0.4) | _ |

AUC: Area under the curve; HeF: Hepatocyte fraction; NLR: Negative likelihood ratio; NPV: Negative predictive value; PLR: Positive likelihood ratio; PPV: Positive predictive value; RE: Reduction rate of T1 relaxation time.

point for each inversion pulse. In addition, Look-Locker is less sensitive to B1 heterogeneity and less prone to error compared with the variable flip angle method[44,45].

Some research into the relationship between RE and liver fibrosis has been conducted. The earliest discussion of the relationship between relative T1 values and fibrosis was reported by Smith *et al*[46] in 1981. However, subsequent studies did not confirm the correlations[47]. Verloh *et al*[26], in a study of the relationship between RE and liver fibrosis, found strong correlations between the uptake characteristics of Gd-EOB-DTPA with RE and the grade of fibrosis/cirrhosis, classified using the Ishak scoring system. The inclusion criteria for this experiment did not limit the type of chronic liver disease that led to liver fibrosis.

Feier *et al*[35] showed a strong correlation between the RE and METAVIR score ($r$ = -0.65), which was consistent with our results ($r$ = -0.773). Among their results, the AUC in the ⩾ F1 and ⩾ F2 stages was higher than our results (⩾ F1: 0.81 *vs* 0.68; ⩾ F2: 0.82 *vs* 0.72). The reasons for this difference in results are as follows. First, Feier *et al*[35] did not focus on liver fibrosis caused by chronic viral hepatitis (CHB, CHC); instead, they included patients with alcoholic liver disease and autoimmune hepatitis leading to liver fibrosis. Second, in our study, the F3 and F4 groups were small, which could have led to bias. Third, RE measurement is relatively simple and direct; however, some disadvantages are also obvious. MRI signal intensity is influenced by many factors, and the collection method of the image may make statistical analysis difficult. Look-Locker sequencing ensures consistent image acquirement and analysis. T1 maps obtained using Look-Locker sequencing may be more robust than simple signal intensity measurements on the hepatobiliary phase[48], as T1 maps are less affected by MR parameters at the same magnetic field strength than signal intensity measurements.

In contrast to the current international consensus on the diagnosis of liver fibrosis using MRE technology, our results showed that, based on Gd-EOB-DTPA-enhanced T1 mapping technology, HeF and METAVIR classification of liver fibrosis were significantly correlated ($r$ = -0.808), although slightly lower than with the MRE technique ($r$ = 0.899). Comparing the AUCs of the ⩾ F1, ⩾ F2, ⩾ F3 and F4 groups, the AUCs for MRE were 0.84, 0.88, 0.93 and 0.92, respectively[49]. Our HeF results were consistent with previous studies.

Compared with MRE technology, which requires a special hardware installation, Gd-EOB-DTPA-enhanced Look-Locker scanning can be operated on standard clinically used MR equipment, an important advantage making it a popular choice. In contrast, the results of studies using the apparent diffusion coefficient (ADC) value in conjunction with DWI to assess hepatic fibrosis were quite different, and the use of ADC values in diagnosis remains controversial. For example, Tokgöz *et al*[50] showed that ADC values in the different grades of fibrosis were not significantly different. A meta-analysis of DWI studies analyzing the use of ADC in

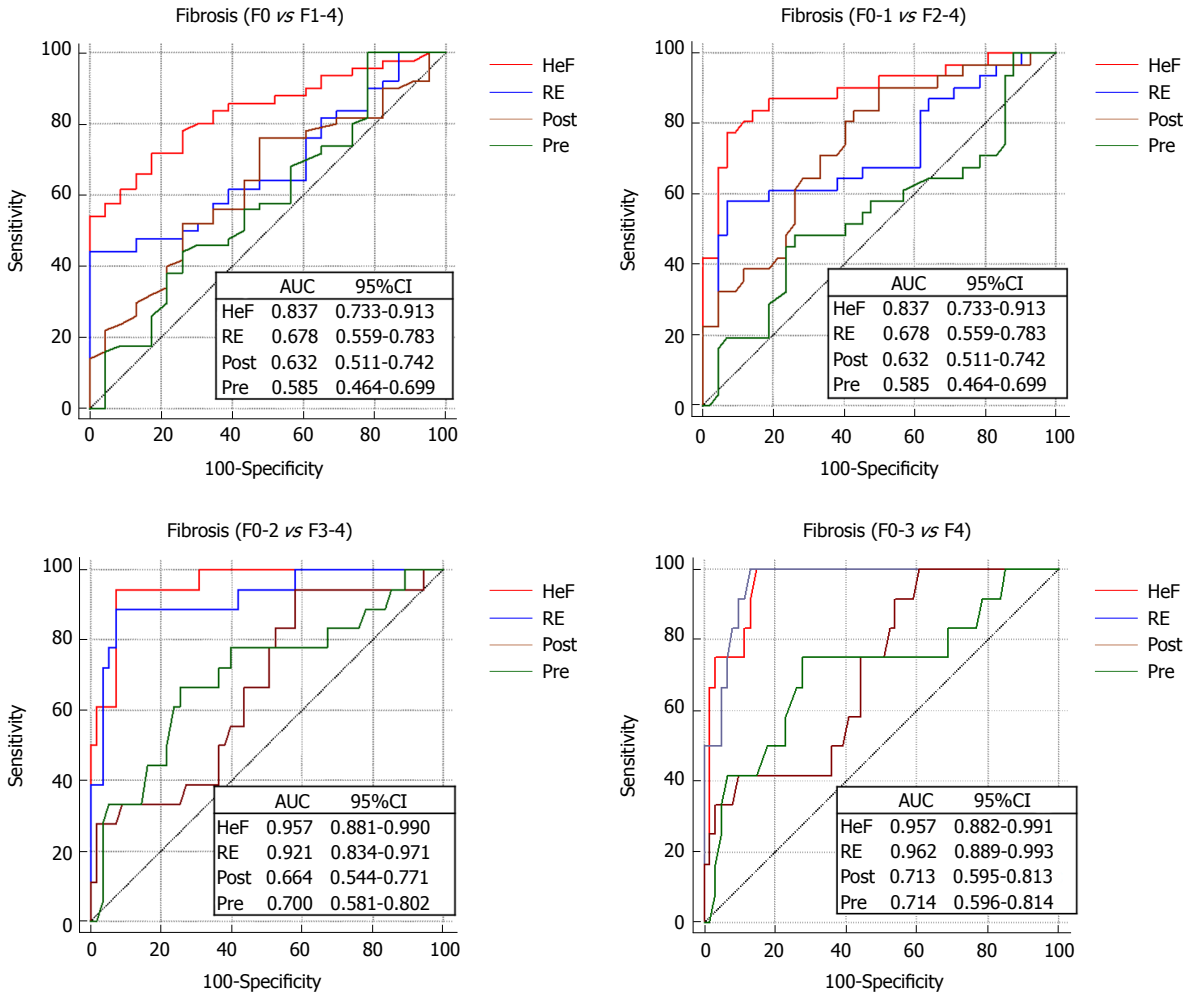


**Figure 6 Comparison of the receiver operating characteristic curves of Pre, Post, RE and HeF for different fibrosis thresholds.** From left to right: F0 *vs* F1-F4 (≥ F1), F0-F1 *vs* F2-F4 (≥ F2), F0-F2 *vs* F3-F4 (≥ F3), and F0-F3 *vs* F4 (≥ F4). The numbers in the boxes indicate the AUC values and 95%CIs. AUC: Area under the receiver operating characteristic curve; CI: Confidence interval; HeF: Hepatocyte fraction; RE: Reduction rate of T1 relaxation time.

liver fibrosis staging included a cumulative total of 613 patients in 10 studies[51]. It reported an AUC of 0.86 for F ≥ 1, 0.83 for F ≥ 2, and 0.86 for F ≥ 3, and concluded that DWI had a good diagnostic value for degree of liver fibrosis. Ding *et al*[52] compared DWI with Gd-EOB-DTPA-enhanced RE in the diagnosis of liver fibrosis; the results showed that RE was better than ADC. In our experiments, HeF was of superior diagnostic value than RE, so we can predict that HeF for liver fibrosis staging is of greater diagnostic value than DWI. Because different b values affect the results of ADC, they cannot be compared between studies because liver fibrosis staging is difficult to establish.

T1 mapping of gadoxetic acid-enhanced MR images using Look-Locker sequencing can be achieved using breath-holding and simplifying the image processing. We believe that this practical method has potential in the quantitative estimate of liver fibrosis and can be used as an important complementary sequence in clinical Gd-EOB-DTPA-enhanced MRI in patients with chronic liver disease.

Our study had some limitations. First, the sample size of this study was small, especially for the F3 stage category. Compared to similar studies which have shown inconsistency in hepatocellular function in the F ≥ 3 stage group (AUC: 0.63, 0.85, 0.87 and 0.93)[53], a larger sample size was needed for the F3 stage category. Second, the study only examined the information obtained at 20 min after Gd-EOB-DTPA administration, and did not analyze HeF measured at other times, such as 5 or 10 min. Third, the Look-Locker sequence was a 2D sequence that did not contain information about the whole liver. When the HeF scan is part of an examination, an enhanced sequence of the whole liver should be added to the scanning protocol because of its value in clinical diagnosis. Furthermore, mismatches between pre- and post-contrast images were observed due to motion and the long gap between scans. To improve accessibility for future clinical use, further development in fast multislice or 3D volume quantitative T1 mapping is needed with liver-specific motion registration.

In conclusion, this study showed a strong correlation between HeF and liver fibrosis stage in CHB and CHC.

Although HeF and RE are used to generate quantitative measurements to distinguish between different grades of liver fibrosis, HeF performed better than RE. This study showed that the T1 mapping-based HeF method is an efficient diagnostic tool for the staging of liver fibrosis.

## ARTICLE HIGHLIGHTS

***Research background***

Chronic hepatitis B/C (CHB/C) are both leading causes of liver-related morbidity and mortality and predisposes patients to liver fibrosis, the excessive accumulation of extracellular matrix proteins. As fibrosis progresses, it leads to cirrhosis and even cancer. Early diagnosis and monitoring of liver fibrosis, and intervention with timely and effective treatments, are critical for patients with liver disease. At present, liver biopsy is the gold standard for diagnosis of liver fibrosis. Invasive methods have a risk of bleeding and increased tissue injury, and the repeatability of the examination is poor. Therefore, noninvasive, comprehensive and accurate methods of diagnosing liver fibrosis are required.

***Research motivation***

Currently, noninvasive methods have been increasingly used, such as serological examination, ultrasound-based elastography, diffusion-weighted imaging, magnetic resonance enterography, and texture analysis. None of these methods can replace the biopsy. T1 mapping *via* the Look-Locker method is one of the fastest approaches to T1 quantification, and is the most time efficient method for T1 mapping and less affected by magnetic resonance parameters than other methods. We proposed a method based on a simple pharmacokinetic model and ΔR1 values to calculate a hepatocyte fraction (HeF). Furthermore, mismatches between pre- and postcontrast images were observed due to motion and the long gap between scans. To improve accessibility for future clinical use, further development in fast multislice or 3D volume quantitative T1 mapping is needed with liver-specific motion registration.

***Research objectives***

We aimed to quantitatively assess the level of hepatic fibrosis in hepatitis B and C patients by calculating the HeF and compare the results with traditional T1-enhanced test parameters. In the future, more imaging methods should be compared with HeF, such as magnetic resonance enterography and diffusion-weighted imaging.

***Research methods***

One hundred and nine patients were included in the study. Magnetic resonance images were obtained with a gadolinium ethoxybenzyl diethylenetriamine pentaacetic acid (Gd-EOB-DTPA)-enhanced 3-Tesla magnetic resonance imaging system, including T1-weighted and Look-Locker sequences for T1 mapping. HeF and relaxation time reduction rate (RE) were calculated for staging hepatic fibrosis. Area under the receiver operating characteristic curve (AUC) was used to compare the diagnostic performance in predicting liver fibrosis between HeF and RE.

***Research results***

We included a total of 73 patients who were deemed eligible for inclusion on histopathological findings. The results of our study indicated that T1 parameters from pre- or postcontrast T1 maps (HeF) and RE had good diagnostic value in the assessment of CHB, CHC and liver fibrosis. HeF and RE both had good diagnostic performance in advanced liver fibrosis and cirrhosis ($\geqslant$ F3 and F4) (AUC > 0.9). In diagnosis at $\geqslant$ F1 and $\geqslant$ F2 stages, HeF was better than RE.

***Research conclusions***

This study showed a strong correlation between HeF and liver fibrosis stage in CHB and CHC. The methods use HeF and RE to generate quantitative measurements to distinguish different grades of liver fibrosis, but HeF performed better than RE. This study showed that the T1 mapping-based HeF method is an efficient diagnostic tool for the staging of liver fibrosis.

***Research perspectives***

Due to the limited number of patients included, further studies are needed to assess the performance of the HeF in hepatic fibrosis. More imaging methods should be compared in the field of liver fibrosis diagnosis.

## REFERENCES


1 **Mohd Hanafiah K**, Groeger J, Flaxman AD, Wiersma ST. Global epidemiology of hepatitis C virus infection: new estimates of age-specific antibody to HCV seroprevalence. *Hepatology* 2013; **57**: 1333-1342 [PMID: 23172780 DOI: 10.1002/hep.26141]

2 **Ott JJ**, Stevens GA, Groeger J, Wiersma ST. Global epidemiology of hepatitis B virus infection: new estimates of age-specific HBsAg seroprevalence and endemicity. *Vaccine* 2012; **30**: 2212-2219 [PMID: 22273662 DOI: 10.1016/j.vaccine.2011.12.116]

3 **Price J**. An update on hepatitis B, D, and E viruses. *Top Antivir Med* 2014; **21**: 157-163 [PMID: 24531556]

4 **Sebastiani G**, Gkouvatsos K, Pantopoulos K. Chronic hepatitis C and liver fibrosis. *World J Gastroenterol* 2014; **20**: 11033-11053 [PMID: 25170193 DOI: 10.3748/wjg.v20.i32.11033]

5 **Bataller R**, Brenner DA. Liver fibrosis. *J Clin Invest* 2005; **115**: 209-218 [PMID: 15690074 DOI: 10.1172/JCI24282]

6 **Suzuki R**, Shin D, Richards-Kortum R, Coghlan L, Bhutani MS. In vivo cytological observation of liver and spleen by using high-resolution microendoscopy system under endoscopic ultrasound guidance: A preliminary study using a swine model. *Endosc Ultrasound* 2016; **5**: 239-242 [PMID: 27503155 DOI: 10.4103/2303-9027.187867]

7 **Oh D**, Seo DW, Hong SM, Song TJ, Park DH, Lee SS, Lee SK, Kim MH. Endoscopic ultrasound-guided fine-needle aspiration can target right liver mass. *Endosc Ultrasound* 2017; **6**: 109-115 [PMID: 28440236 DOI: 10.4103/2303-9027.204813]

8 **Hassan GM**, Paquin SC, Sahai AV. Large liver abscess after endoscopic ultrasound-guided fiducial placement. *Endosc Ultrasound* 2017; **6**: 418-419 [PMID: 28836513 DOI: 10.4103/eus.eus_17_17]

9 **Choi JH**, Seo DW. Applications of contrast-enhanced harmonic endoscopic ultrasound on biliary, focal liver lesions and vascular diseases. *Endosc Ultrasound* 2017; **6**: 21-24 [PMID: 28218196 DOI: 10.4103/2303-9027.200211]

10 **Guo J**, Liu Z, Sun S, Qi Y. Biliary intraductal papillary-mucinous neoplasm in the left hepatic lobe diagnosed by endoscopic ultrasonography: Report of a case. *Endosc Ultrasound* 2016; **5**: 274-275 [PMID: 27503163 DOI: 10.4103/2303-9027.187894]

11 **Bravo AA**, Sheth SG, Chopra S. Liver biopsy. *N Engl J Med* 2001; **344**: 495-500 [PMID: 11172192 DOI: 10.1056/NEJM200102153440706]

12 **Biermann K**, Lozano Escario MD, Hébert-Magee S, Rindi G, Doglioni C. How to prepare, handle, read, and improve EUS-FNA and fine-needle biopsy for solid pancreatic lesions: The pathologist' s role. *Endosc Ultrasound* 2017; **6**: S95-S98 [PMID: 29387701 DOI: 10.4103/eus.eus_71_17]

13 **Chin JL**, Pavlides M, Moolla A, Ryan JD. Non-invasive Markers of Liver Fibrosis: Adjuncts or Alternatives to Liver Biopsy? *Front Pharmacol* 2016; **7**: 159 [PMID: 27378924 DOI: 10.3389/fphar.2016.00159]

14 **Afdhal NH**, Bacon BR, Patel K, Lawitz EJ, Gordon SC, Nelson DR, Challies TL, Nasser I, Garg J, Wei LJ, McHutchison JG. Accuracy of fibroscan, compared with histology, in analysis of liver fibrosis in patients with hepatitis B or C: a United States multicenter study. *Clin Gastroenterol Hepatol* 2015; **13**: 772-9.e1-3 [PMID: 25528010 DOI: 10.1016/j.cgh.2014.12.014]

15 **Palmucci S**, Cappello G, Attinà G, Fuccio Sanzà G, Foti PV, Ettorre GC, Milone P. Diffusion-weighted MRI for the assessment of liver fibrosis: principles and applications. *Biomed Res Int* 2015; **2015**: 874201 [PMID: 25866819 DOI: 10.1155/2015/874201]

16 **Wang J**, Malik N, Yin M, Smyrk TC, Czaja AJ, Ehman RL, Venkatesh SK. Magnetic resonance elastography is accurate in detecting advanced fibrosis in autoimmune hepatitis. *World J Gastroenterol* 2017; **23**: 859-868 [PMID: 28223730 DOI: 10.3748/wjg.v23.i5.859]

17 **Xie Y**, Zhang H, Jin C, Wang X, Wang X, Chen J, Xu Y. Gd-EOB-DTPA-enhanced T1ρ imaging vs diffusion metrics for assessment liver inflammation and early stage fibrosis of nonalcoholic steatohepatitis in rabbits. *Magn Reson Imaging* 2018; **48**: 34-41 [PMID: 29278765 DOI: 10.1016/j.mri.2017.12.017]

18 **House MJ**, Bangma SJ, Thomas M, Gan EK, Ayonrinde OT, Adams LA, Olynyk JK, St Pierre TG. Texture-based classification of liver fibrosis using MRI. *J Magn Reson Imaging* 2015; **41**: 322-328 [PMID: 24347292 DOI: 10.1002/jmri.24536]

19 **Dahlqvist Leinhard O**, Dahlström N, Kihlberg J, Sandström P, Brismar TB, Smedby O, Lundberg P. Quantifying differences in hepatic uptake of the liver specific contrast agents Gd-EOB-DTPA and Gd-BOPTA: a pilot study. *Eur Radiol* 2012; **22**: 642-653 [PMID: 21984449 DOI: 10.1007/s00330-011-2302-4]

20 **Kogita S**, Imai Y, Okada M, Kim T, Onishi H, Takamura M, Fukuda K, Igura T, Sawai Y, Morimoto O, Hori M, Nagano H, Wakasa K, Hayashi N, Murakami T. Gd-EOB-DTPA-enhanced magnetic resonance images of hepatocellular carcinoma: correlation with histological grading and portal blood flow. *Eur Radiol* 2010; **20**: 2405-2413 [PMID: 20490505 DOI: 10.1007/s00330-010-1812-9]

21 **Motosugi U**, Ichikawa T, Sou H, Sano K, Tominaga L, Muhi A, Araki T. Distinguishing hypervascular pseudolesions of the liver from hypervascular hepatocellular carcinomas with gadoxetic acid-enhanced MR imaging. *Radiology* 2010; **256**: 151-158 [PMID: 20574092 DOI: 10.1148/radiol.10091885]

22 **Pan S**, Guo Q. Endoscopic ultrasonography versus magnetic resonance cholangiopancreatography for suspected choledocholithiasis: Comments from the radiologists'. *Endosc Ultrasound* 2016; **5**: 129-131 [PMID: 27080612 DOI: 10.4103/2303-9027.180477]

23 **Leonhardt M**, Keiser M, Oswald S, Kühn J, Jia J, Grube M, Kroemer HK, Siegmund W, Weitschies W. Hepatic uptake of the magnetic resonance imaging contrast agent Gd-EOB-DTPA: role of human organic anion transporters. *Drug Metab Dispos* 2010; **38**: 1024-1028 [PMID: 20406852 DOI: 10.1124/dmd.110.032862]

24 **Juluru K**, Talal AH, Yantiss RK, Spincemaille P, Weidman EK, Giambrone AE, Jalili S, Sourbron SP, Dyke JP. Diagnostic accuracy of intracellular uptake rates calculated using dynamic Gd-EOB-DTPA-enhanced MRI for hepatic fibrosis stage. *J Magn Reson Imaging* 2017; **45**: 1177-1185 [PMID: 27527820 DOI: 10.1002/jmri.25431]

25 **Tsuda N**, Matsui O. Cirrhotic rat liver: reference to transporter activity and morphologic changes in bile canaliculi--gadoxetic acid-enhanced MR imaging. *Radiology* 2010; **256**: 767-773 [PMID: 20663976 DOI: 10.1148/radiol.10092065]

26 **Verloh N**, Utpatel K, Haimerl M, Zeman F, Fellner C, Fichtner-Feigl S, Teufel A, Stroszczynski C, Evert M, Wiggermann P. Liver fibrosis and Gd-EOB-DTPA-enhanced MRI: A histopathologic correlation. *Sci Rep* 2015; **5**: 15408 [PMID: 26478097 DOI: 10.1038/srep15408]

27 **Kim KA**, Park MS, Kim IS, Kiefer B, Chung WS, Kim MJ, Kim KW. Quantitative evaluation of liver cirrhosis using T1 relaxation time with 3 tesla MRI before and after oxygen inhalation. *J Magn Reson Imaging* 2012; **36**: 405-410 [PMID: 22392835 DOI: 10.1002/jmri.23620]

28 **Li Z**, Sun J, Hu X, Huang N, Han G, Chen L, Zhou Y, Bai W, Yang X. Assessment of liver fibrosis by variable flip angle T1 mapping at 3.0T. *J Magn Reson Imaging* 2016; **43**: 698-703 [PMID: 26267123 DOI: 10.1002/jmri.25030]

29 **Crawley AP**, Henkelman RM. A comparison of one-shot and recovery methods in T1 imaging. *Magn Reson Med* 1988; **7**: 23-34 [PMID: 3386519]

30 **Yoon JH**, Lee JM, Paek M, Han JK, Choi BI. Quantitative assessment of hepatic function: modified look-locker inversion recovery (MOLLI) sequence for T1 mapping on Gd-EOB-DTPA-enhanced liver MR imaging. *Eur Radiol* 2016; **26**: 1775-1782 [PMID: 26373756 DOI: 10.1007/s00330-015-3994-7]

31 **Nacif MS**, Turkbey EB, Gai N, Nazarian S, van der Geest RJ, Noureldin RA, Sibley CT, Ugander M, Liu S, Arai AE, Lima JA, Bluemke DA. Myocardial T1 mapping with MRI: comparison of look-locker and MOLLI sequences. *J Magn Reson Imaging* 2011; **34**: 1367-1373 [PMID: 21954119 DOI: 10.1002/jmri.22753]

32 **Bedossa P**, Poynard T. An algorithm for the grading of activity in chronic hepatitis C. The METAVIR Cooperative Study Group. *Hepatology* 1996; **24**: 289-293 [PMID: 8690394 DOI: 10.1002/hep.510240201]

33 Intraobserver and interobserver variations in liver biopsy interpretation in patients with chronic hepatitis C. The French METAVIR Cooperative Study Group. *Hepatology* 1994; **20**: 15-20 [PMID: 8020885]

34 **DeLong ER**, DeLong DM, Clarke-Pearson DL. Comparing the areas under two or more correlated receiver operating characteristic curves: a nonparametric approach. *Biometrics* 1988; **44**: 837-845 [PMID: 3203132]

35 **Feier D**, Balassy C, Bastati N, Stift J, Badea R, Ba-Ssalamah A. Liver fibrosis: histopathologic and biochemical influences on diagnostic efficacy of hepatobiliary contrast-enhanced MR imaging in staging. *Radiology* 2013; **269**: 460-468 [PMID: 23878281 DOI: 10.1148/radiol.13122482]

36 **Nishie A**, Asayama Y, Ishigami K, Tajima T, Kakihara D, Nakayama T, Takayama Y, Okamoto D, Taketomi A, Shirabe K, Fujita N, Obara M, Yoshimitsu K, Honda H. MR prediction of liver fibrosis using a liver-specific contrast agent: Superparamagnetic iron oxide versus Gd-EOB-DTPA. *J Magn Reson Imaging* 2012; **36**: 664-671 [PMID: 22532503 DOI: 10.1002/jmri.23691]

37 **Watanabe H**, Kanematsu M, Goshima S, Kondo H, Onozuka M, Moriyama N, Bae KT. Staging hepatic fibrosis: comparison of gadoxetate disodium-enhanced and diffusion-weighted MR imaging--preliminary observations. *Radiology* 2011; **259**: 142-150 [PMID: 21248234 DOI: 10.1148/radiol.10100621]

38 **Chen BB**, Hsu CY, Yu CW, Wei SY, Kao JH, Lee HS, Shih TT. Dynamic contrast-enhanced magnetic resonance imaging with Gd-EOB-DTPA for the evaluation of liver fibrosis in chronic hepatitis patients. *Eur Radiol* 2012; **22**: 171-180 [PMID: 21879400 DOI: 10.1007/s00330-011-2249-5]

39 **Katsube T**, Okada M, Kumano S, Hori M, Imaoka I, Ishii K, Kudo M, Kitagaki H, Murakami T. Estimation of liver function using T1 mapping on Gd-EOB-DTPA-enhanced magnetic resonance imaging. *Invest Radiol* 2011; **46**: 277-283 [PMID: 21343827 DOI: 10.1097/RLI.0b013e318200f67d]

40 **Kamimura K**, Fukukura Y, Yoneyama T, Takumi K, Tateyama A, Umanodan A, Shindo T, Kumagae Y, Ueno S, Koriyama C, Nakajo M. Quantitative evaluation of liver function with T1 relaxation time index on Gd-EOB-DTPA-enhanced MRI: comparison with signal intensity-based indices. *J Magn Reson Imaging* 2014; **40**: 884-889 [PMID: 24677659 DOI: 10.1002/jmri.24443]

41 **Yang L**, Ding Y, Rao S, Chen C, Wu L, Sheng R, Fu C, Zeng M. Staging liver fibrosis in chronic hepatitis B with $T_1$ relaxation time index on gadoxetic acid-enhanced MRI: Comparison with aspartate aminotransferase-to-platelet ratio index and FIB-4. *J Magn Reson Imaging* 2017; **45**: 1186-1194 [PMID: 27563840 DOI: 10.1002/jmri.25440]

42 **Banerjee R**, Pavlides M, Tunnicliffe EM, Piechnik SK, Sarania N, Philips R, Collier JD, Booth JC, Schneider JE, Wang LM, Delaney DW, Fleming KA, Robson MD, Barnes E, Neubauer S. Multiparametric magnetic resonance for the non-invasive diagnosis of liver disease. *J Hepatol* 2014; **60**: 69-77 [PMID: 24036007 DOI: 10.1016/j.jhep.2013.09.002]

43 **Sheng RF**, Wang HQ, Yang L, Jin KP, Xie YH, Fu CX, Zeng MS. Assessment of liver fibrosis using T1 mapping on Gd-EOB-DTPA-enhanced magnetic resonance. *Dig Liver Dis* 2017; **49**: 789-795 [PMID: 28237298 DOI: 10.1016/j.dld.2017.02.006]

44 **Li W**, Griswold M, Yu X. Rapid T1 mapping of mouse myocardium with saturation recovery Look-Locker method. *Magn Reson Med* 2010; **64**: 1296-1303 [PMID: 20632410 DOI: 10.1002/mrm.22544]

45 **Liberman G**, Louzoun Y, Ben Bashat D. $T_1$ mapping using variable flip angle SPGR data with flip angle correction. *J Magn Reson Imaging* 2014; **40**: 171-180 [PMID: 24990618 DOI: 10.1002/jmri.24373]

46 **Smith FW**, Mallard JR, Reid A, Hutchison JM. Nuclear magnetic resonance tomographic imaging in liver disease. *Lancet* 1981; **1**: 963-966 [PMID: 6112385]
47 **Aisen AM**, Doi K, Swanson SD. Detection of liver fibrosis with magnetic cross-relaxation. *Magn Reson Med* 1994; **31**: 551-556 [PMID: 8015410]
48 **Motosugi U**, Ichikawa T, Sou H, Sano K, Tominaga L, Kitamura T, Araki T. Liver parenchymal enhancement of hepatocyte-phase images in Gd-EOB-DTPA-enhanced MR imaging: which biological markers of the liver function affect the enhancement? *J Magn Reson Imaging* 2009; **30**: 1042-1046 [PMID: 19856436 DOI: 10.1002/jmri.21956]
49 **Singh S**, Venkatesh SK, Wang Z, Miller FH, Motosugi U, Low RN, Hassanein T, Asbach P, Godfrey EM, Yin M, Chen J, Keaveny AP, Bridges M, Bohte A, Murad MH, Lomas DJ, Talwalkar JA, Ehman RL. Diagnostic performance of magnetic resonance elastography in staging liver fibrosis: a systematic review and meta-analysis of individual participant data. *Clin Gastroenterol Hepatol* 2015; **13**: 440-451.e6 [PMID: 25305349 DOI: 10.1016/j.cgh.2014.09.046]
50 **Tokgöz Ö**, Unal I, Turgut GG, Yildiz S. The value of liver and spleen ADC measurements in the diagnosis and follow up of hepatic fibrosis in chronic liver disease. *Acta Clin Belg* 2014; **69**: 426-432 [PMID: 25103596 DOI: 10.1179/2295333714y.0000000062]
51 **Wang QB**, Zhu H, Liu HL, Zhang B. Performance of magnetic resonance elastography and diffusion-weighted imaging for the staging of hepatic fibrosis: A meta-analysis. *Hepatology* 2012; **56**: 239-247 [PMID: 22278368 DOI: 10.1002/hep.25610]
52 **Ding Y**, Rao SX, Zhu T, Chen CZ, Li RC, Zeng MS. Liver fibrosis staging using T1 mapping on gadoxetic acid-enhanced MRI compared with DW imaging. *Clin Radiol* 2015; **70**: 1096-1103 [PMID: 26164421 DOI: 10.1016/j.crad.2015.04.014]
53 **Petitclerc L**, Sebastiani G, Gilbert G, Cloutier G, Tang A. Liver fibrosis: Review of current imaging and MRI quantification techniques. *J Magn Reson Imaging* 2017; **45**: 1276-1295 [PMID: 27981751 DOI: 10.1002/jmri.25550]

**P- Reviewer**: McHenry L, Mulvihill SJ, Otto G
**S- Editor**: Gong ZM **L- Editor**: Filipodia **E- Editor**: Huang Y

Published by **Baishideng Publishing Group Inc**
7901 Stoneridge Drive, Suite 501, Pleasanton, CA 94588, USA
Telephone: +1-925-223-8242
Fax: +1-925-223-8243
E-mail: bpgoffice@wjgnet.com
Help Desk: http://www.f6publishing.com/helpdesk
http://www.wjgnet.com

ISSN 1007-9327